2014

# The HMGB1/RAGE inflammatory pathway promotes pancreatic tumor growth by regulating mitochondrial bioenergetics

R. Kang

D. Tang

N. E. Schapiro

T. Loux

K. M. Livesey

***See next page for additional authors***

**Authors**
R. Kang, D. Tang, N. E. Schapiro, T. Loux, K. M. Livesey, T. R. Billiar, H. Wang, B. Van Houten, M. T. Lotze, and H. J. Zeh

Published in final edited form as:
*Oncogene*. 2014 January 30; 33(5): 567–577. doi:10.1038/onc.2012.631.

# The HMGB1/RAGE inflammatory pathway promotes pancreatic tumor growth by regulating mitochondrial bioenergetics

**R Kang**[1], **D Tang**[1], **NE Schapiro**[1], **T Loux**[1], **KM Livesey**[1], **TR Billiar**[1], **H Wang**[2], **B Van Houten**[3], **MT Lotze**[1], and **HJ Zeh**[1]

[1]Department of Surgery, Hillman Cancer Center, University of Pittsburgh Cancer Institute, Pittsburgh, PA, USA

[2]North Shore University Hospital, New York University School of Medicine, Manhasset, NY, USA

[3]Laboratory of Molecular and Cell Biology Program, Hillman Cancer Center, University of Pittsburgh Cancer Institute, University of Pittsburgh, Pittsburgh, PA, USA

## Abstract

Tumor cells require increased adenosine triphosphate (ATP) to support anabolism and proliferation. The precise mechanisms regulating this process in tumor cells are unknown. Here, we show that the receptor for advanced glycation endproducts (RAGE) and one of its primary ligands, high-mobility group box 1 (HMGB1), are required for optimal mitochondrial function within tumors. We found that RAGE is present in the mitochondria of cultured tumor cells as well as primary tumors. RAGE and HMGB1 coordinately enhanced tumor cell mitochondrial complex I activity, ATP production, tumor cell proliferation and migration. Lack of RAGE or inhibition of HMGB1 release diminished ATP production and slowed tumor growth *in vitro* and *in vivo*. These findings link, for the first time, the HMGB1–RAGE pathway with changes in bioenergetics. Moreover, our observations provide a novel mechanism within the tumor microenvironment by which necrosis and inflammation promote tumor progression.

### Keywords

HMGB1; RAGE; pancreatic cancer; inflammation; mitochondria; ATP

## INTRODUCTION

Cancer can be defined by several critical alterations in normal cellular physiology, including uncontrolled growth, immortality, evasion of apoptosis and ability to invade other tissues.[1] More recently, it has become clear that two additional hallmarks should be included in the setting of adult neoplasms— inflammation arising from necrosis and altered cellular metabolism.[2,3] Here, we demonstrate a link between cancer necrosis, resultant inflammatory signals within the pancreatic tumor microenvironment and altered cellular metabolism. High-mobility group box 1 (HMGB1) and the receptor for advanced glycation endproducts (RAGE) are critical for enhanced tumor cell mitochondrial production of adenosine



Correspondence: Dr D Tang or Dr HJ Zeh or MT Lotze, Department of Surgery, Hillman Cancer Center, University of Pittsburgh Cancer Institute, 5117 Center Avenue, Pittsburgh, PA 15219, USA. tangd2@upmc.edu or lotzemt@upcm.edu or zehh@upmc.edu.

**CONFLICT OF INTEREST**

The authors declare no conflict of interest.

triphosphate (ATP) and ATP-dependent functions, including proliferation, migration and *in vivo* orthotopic transplantation models of pancreatic tumor growth.

HMGB1, a chromatin-associated nuclear protein and extracellular damage-associated molecular-pattern molecule, is overexpressed in tumor cells and triggers inflammation, cell migration and tumor metastasis following release into the extracellular space.[4,5] We have previously demonstrated that HMGB1, through one of its primary receptors, RAGE, promotes tumor cell survival following genomic or metabolic stress.[6,7] HMGB1 knockout mice demonstrate profound disturbances in metabolism, succumbing during the neonatal period to refractory hypoglycemia.[8] The pancreas is an organ regulating host metabolism, harboring pancreatic exocrine cells producing digestive enzymes, ductal cells involved with their transport, and the endocrine cells that produce predominantly insulin and glucagon. Our recent findings demonstrated that RAGE modulates crosstalk between pro-survival pathways, IL6-pSTAT3 and autophagy, in pancreatic ductal adenocarcinoma tumor cells, and contributes to early pancreatic intraepithelial neoplasia formation.[9] Here, we hypothesized that signaling through the HMGB1/RAGE pathway would enhance pancreatic ductal tumor cell survival and protect them from cytotoxic insult through linkage to altered cellular metabolism.

## RESULTS

### Exogenous HMGB1 promotes increased ATP production in human and murine pancreatic tumor cell lines

We stimulated several pancreatic tumor cell lines with highly purified low endotoxin HMGB1 (endotoxin ≤3.1 EU/ml). HMGB1 promoted ATP production and proliferation in human and murine pancreatic tumor cell lines in a time- and dose-dependent manner (Figure 1a). This observation was not limited to pancreatic tumor cell lines, as HMGB1 also promoted ATP production in human colon cancer (HCT116), leukemia (HL-60, Jurkat) and lung cancer cells (A549) (Supplementary Figure S1). The histone deacetylase inhibitor, trichostatin A, completely inhibited HMGB1-induced cell proliferation, but not ATP production (Figure 1b). These findings suggest that HMGB1-induced ATP production is not solely dependent on cellular proliferation. Release of HMGB1 by lysed ‘necrotic,’ but not ‘apoptotic’ cells triggers inflammation.[10] As expected, HMGB1 wild-type ‘necrotic’ murine embryonic fibroblasts (MEFs) triggered production of ATP, whereas wild-type apoptotic MEFs were much less effective (Figure 1c). Significantly, $HMGB1^{-/-}$ MEFs (Figure 1c) and necrotic MEFs in which HMGB1 activity was inhibited with a neutralizing antibody (Figure 1d, left panel) were also unable to enhance ATP generation. Extracellular HMGB1 forms complexes with pathogen-associated molecular pattern molecules such as lipopolysaccharide and cytokines such as interleukin-1β+ (IL-1β), thereby promoting inflammation.[11] HMGB1-induced ATP production is not dependent on binding to DNA, IL-1 β or interferon (IFN)-γ (Figure 1d, right panel), based on neutralization studies. To determine whether ATP production is required for other aspects of HMGB1 function, we treated cells with a mitochondrial complex I inhibitor, rotenone (Rote). Rote (500 $n_M$–2 $\mu_M$) treatment dose dependently limited ATP production (Figure 1e) induced by exogenous HMGB1. Nuclear factor-κB (NF-κB) is a central mediator of inflammation,[12] cell migration[13] and tumor cell growth. We observed that Rote also inhibited HMGB1-mediated NF-κB activity, cell migration and division (Figure 1e). shRNA knockdown of the p65 subunit of NF-κB, however, inhibited HMGB1-induced cell proliferation, but not ATP production in pancreatic cancer cells (Figure 1f), suggesting that NF-κB is not required for HMGB1-mediated ATP production. In addition, in preliminary observations we also observed that fresh human pancreatic tumor biopsies demonstrate increased HMGB1, ATP

and CD11b-positive inflammatory cells when compared to the adjacent control pancreas (Supplementary Figure S2).

## Exogenous HMGB1 increases tumor cell ATP production through RAGE

To determine which HMGB1 receptor is responsible for mediating enhanced ATP production, we used specific shRNA and antibodies directed against known HMGB1 receptors. Targeted interference with signaling through RAGE, but not TLR-2, −4 nor CD24, suppressed HMGB1-induced ATP production (Figure 2a). Complex I is the first step in the mitochondrial ATP synthetic pathway. Targeting RAGE suppressed complex I activity but not the abundance of the complex I subunits NDUFA9 and GRIM-19 (Figure 2b). RAGE shRNA and neutralizing antibodies decreased HMGB1-induced ATP production and complex I activity in individual tumor cell lines (Figures 2a and b).

The cytosolic tail of RAGE (‘cyt-RAGE’) is essential for RAGE-dependent signal transduction.[14,15] We found that overexpression of the short cyt-RAGE increased basal and HMGB1-induced ATP production in RAGE knockdown Panc02 cells (Figure 2c). Indomethacin, an inhibitor of caveolin-mediated endocytic HMGB1 uptake,[16] significantly reversed HMGB1-mediated ATP production and cell proliferation when cyt-RAGE is overexpressed in RAGE knockdown cells (Figure 2c). Structure–function studies have demonstrated that the cytosolic tail is essential for RAGE-mediated intracellular signal activation such as NF-κB, MEK–ERK–MAPK or mTOR.[17,18] To explore whether these signals are also required for cyt-RAGE-mediated ATP production in Panc02 cells, we treated these cells with a microtubule-associated protein kinase (MEK) inhibitor (for example, U0126), an NF-κB inhibitor (for example, Bay 11-7085) or an mTOR inhibitor (for example, Rapamycin). Only U0126 inhibited cyt-RAGE-mediated ATP production in RAGE knockdown cells (Figure 2c). Moreover, U0126 inhibited HMGB1-mediated ATP production when cyt-RAGE and full-RAGE is overexpressed in RAGE wild-type Panc02 cells (Figure 2d). These studies suggest that the MEK–ERK–MAPK pathway is involved in RAGE-mediated ATP production.

## RAGE is expressed in mitochondria

RAGE is overexpressed in many different types of cancer, including pancreatic tumors.[7,18] We determined the level of RAGE in several pancreatic tumor cell lines (Panc02, Panc2.03 and Panc3.27), as well as normal pancreatic tissues of mice and humans. RAGE was detected in both the mitochondrial and cytoplasmic fractions (Figure 3a) of cells. Colocalization of mitochondria and RAGE is observed in Panc02 tumor cells as well as in mouse pancreas, lung, heart and liver cells (Supplementary Figure S3). In addition, RAGE co-localizes with mitochondria in human pancreatic tumor tissues as determined by confocal microscopy (Supplementary Figure S4). To distinguish mitochondrial RAGE (mitRAGE) from that arising from contamination with the cytoplasm, we precipitated proteins of purified mitochondria and cytosol in parallel with RAGE, tubulin and mitochondrial HSP70 (mitHSP70). The ratio of RAGE to tubulin in the cytoplasm does not correlate with increasing amounts of purified mitochondria (Figure 3b), but rather mitRAGE to mitHSP70 ratio increases in a dose-dependent fashion, suggesting that presence of RAGE detected within the mitochondria is not due to cytosolic contamination. To determine whether mitRAGE is located in the outer membrane of the mitochondrion, we incubated pancreatic tumor cell mitochondria with proteinase K in the presence or absence of triton X-100.[19] RAGE, retinoid-IFN-induced mortality-19 (GRIM-19, an inner membrane protein), and mitochondrial cytochrome oxidase IV (an inner membrane protein) are resistant to proteinase K, whereas Bcl-2 (an outer membrane protein) is degraded (Figure 3c). As a positive control, when proteinase K is added to mitochondria in the presence of triton X-100, all of the proteins are degraded. Thus, RAGE is likely located in the intermembrane

space, the inner mitochondrial membrane or the matrix, but not in or associated with the outer membrane.

## RAGE localizes to complex I of the mitochondria

To understand how RAGE positively regulates ATP production, we assessed RAGE within immunoprecipitates of mitochondrial extracts prepared from pancreatic tumor cells with the use of capture reagents for individual components of complex I, II, III or IV of the mitochondrial electron transport chain (Figure 3d). To ensure antibody specificity, the blots were also probed for known components of complex I (NDUFA9), complex II (Fb subunit), complex III (core protein 2) and complex IV (subunit 1). Immunoprecipitates of complex I and II contain RAGE, whereas immunoreactive RAGE is not detected in immunoprecipitates using the IgG, complex III or IV antibody (Figure 3d). Notably, HMGB1 enhanced the expression of mitRAGE in immunoprecipitates of complex I and II, but not III and IV.

The mitochondrial electron transport chain in the mitochondrion is the site of oxidative phosphorylation (OXPHOS) within eukaryotic cells. Post-glycolytic reactions also take place within the mitochondria in eukaryotes, using imported pyruvate to generate acetyl-CoA for further biogenesis. To elucidate how RAGE regulates mitochondrial bioenergetics, we assessed real-time OXPHOS by determining the oxygen consumption rate (OCR) and glycolysis by measuring the extracellular acidification rate (ECR) using an extracellular flux analyzer[20] in RAGE wild-type and RAGE knockdown Panc02 cells (Figure 3e). Analysis of OCR and ECR was performed in the presence of four individual inhibitors: (1) oligomycin, which inhibits mitochondrial ATP synthesis, (2) p-trifluoromethoxy carbonyl cyanide phenyl hydrazone, which uncouples OXPHOS, revealing reserve capacity within the mitochondria, (3) 2-deoxyglucose, which inhibits hexokinase in the glycolytic pathway and (4) Rote, which inhibits complex I in the respiratory chain. Addition of HMGB1 to wild-type Panc02 tumor cells induced an increase in both OCR and ECR. Knockdown of RAGE in these tumor cells led to a decrease in basal OCR and ECR that was not improved by the addition of HMGB1. Together, these findings support the notion that RAGE has a critical role in maintaining tumor cell bioenergetics.

## Exogenous HMGB1 promotes mitochondrial localization of RAGE that is associated with phosphorylation of RAGE and interaction with p-ERK1/2

We next examined the effect of exogenous HMGB1 on RAGE expression in the mitochondria. We first observed that human pancreatic tumors demonstrated a two-fold increase in overall RAGE expression and a 5.8-fold increase in mitRAGE (Figure 3f) when compared to the adjacent control pancreatic tissue. We hypothesized that HMGB1 was responsible for the increased RAGE observed in mitochondria in tumor tissue. To test this, we treated human pancreatic tumor cell lines with HMGB1. We observed a dose- and time-dependent increase in mitRAGE (Figure 3g and Supplementary Figure S5). Similarly, HMGB1 within necrotic cell lysates increased the pancreatic tumor cell expression of RAGE, NF-κB activity and cell migration (Supplementary Figure S6).

Regulation of mitochondrial proteins, including complex I, by phosphorylation is commonly identified in the maintenance of mitochondrial processes, including OXPHOS.[21] To determine whether RAGE is a phosphoprotein, cell extracts were immunoprecipitated with antiRAGE antibody and analyzed with an antiphosphoserine antibody. The amount of phosphorylated RAGE (p-RAGE) and complex I (p-CxI) increased following HMGB1 treatment (Figure 4a). HMGB1 triggers extracellular signal-regulated kinase 1/2 phosphorylation (p-ERK1/2) and activation in several cell types[22,23] (Figure 4a). To determine whether HMGB1 activates the ERK1/2 pathway, we treated pancreatic tumor

cells with the ERK inhibitors (U0126 and PD98059) or knocked-down MEK2, which functions as an immediate upstream activating kinase of ERK, using specific siRNA. Notably, ERK inhibitors (Figure 4a) and MEK2 siRNA (Figure 4b) inhibited HMGB1-induced p-RAGE and p-CxI, as well as mitRAGE and ATP production. RAGE is indeed a positive regulator of the ERK pathway.[17,18] Similarly, RAGE knockdown in pancreatic tumor cells blocked damageassociated molecular pattern molecules (such as HMGB1), pathogen-associated molecular pattern molecules (such as lipopolysaccharide, for example, cytokines such as tTNF-α) and chemotherapy (for example, oxaliplatin and melphalan)-induced phosphorylation of ERK1/2 (Figure 4c). Thus, ERK promotes RAGE phosphorylation following HMGB1 stimulation, and RAGE is required for generation of p-ERK1/2 following stress. This suggests that there may be a direct interaction between RAGE and p-ERK1/ 2, which mediates and promotes feed forward/coupled phosphorylation activity.

To confirm that there is a direct interaction between RAGE and p-ERK1/2 in cells, immunoprecipitation followed by immunoblotting analysis were carried out using anti-RAGE and anti-p-ERK1/2 antibodies. A p-ERK–RAGE complex is found in cells following HMGB1 stimulation by co-immunoprecipitation assay (Figure 4d). The ERK inhibitor U0126 also blocked p-ERK1/2 binding to RAGE (Figure 4d). The cyt-RAGE, but not extracellular (ex-RAGE) or transmembrane-spanning domain (m-RAGE), is required for binding p-ERK1/2 following HMGB1 stimulation (Figure 4e). p-RAGE translocated from the cytoplasm to the mitochondria following HMGB1 treatment (Figure 4f). To determine whether RAGE phosphorylation and accumulation within the mitochondria required new protein synthesis, we treated cells with the protein biosynthesis inhibitor cycloheximide (Figure 4g). Cycloheximide inhibited HMGB1-induced RAGE phosphorylation and accumulation within the mitochondria. Moreover, we demonstrated that HMGB1 induced translocation to the mitochondria of full-length RAGE, but not transmembrane RAGE (exm-RAGE) (Figure 4h). These findings suggest that RAGE phosphorylation and accumulation within the mitochondria requires new protein synthesis, but not translocation of the plasma membrane portion of RAGE to the mitochondria.

The C-terminal cytoplasmic domain of mouse RAGE has two potential phosphorylation sites: Ser377 and Ser399. We assessed these residues as phosphorylation sites promoting RAGE-mediated ATP production. We transfected expression plasmids into tumor cells that expressed either wild-type RAGE or alanine for serine mutants (S377A, S399A, S377A/S399A). When compared with wild-type RAGE, S377A and S377A/S399A mutants impaired both basal and HMGB1-mediated localization of mitRAGE, p-CxI and subsequent ATP production, whereas S399A was equally effective as the wild type (Figure 4i). Thus, it appears that the mitochondrial localization signal, Ser377 of RAGE, is required for HMGB1-mediated RAGE activation within the mitochondria.

Targeting the HMGB1/RAGE axis decreases in vivo tumor growth To determine whether blocking the HMGB1–RAGE axis decreases tumor growth *in vivo*, we inoculated C57/BL6 mice subcutaneously with Panc02 tumor cells, following transfection with control or RAGE-specific shRNA. We then treated them with ethyl pyruvate (EP), a pharmacological inhibitor of nuclear HMGB1 to cytosol translocation and secretion.[24] *In vivo*, growth of RAGE knockdown tumor cells was significantly slower than controls (Figure 5a). Growth of control shRNA-transfected tumors was significantly inhibited at an effective dose of EP (40 mg/kg), but not in the RAGE shRNA group (Figure 5a). We also monitored markers of apoptosis (cleaved-polyADP-ribose polymerase (PARP), expression of B-cell lymphoma 2 (Bcl-2)), inflammation (p-NFκB p65 (p-p65)) and autophagy (microtubule-associated protein light chain 3 (LC3)-I/II) on day 42. Targeted interference of HMGB1/RAGE signaling increased markers of apoptosis (PARP) and decreased markers of inflammation (p-

p65), autophagy (LC3-II), ATP production and complex I activity (Figure 5b). *In vitro*, EP at a dose of 10 $m_M$ inhibits HMGB1 release.[24] Low-dose EP (10 $m_M$) did not influence cellular proliferation (Figure 5c). However, high-dose EP (for example,40 $m_M$) significantly inhibited proliferation (Figure 5c). Similarly, the complex I inhibitor Rote resulted in a dose-dependent inhibition of HMGB1-induced tumor cell proliferation (Figure 1e). In addition, the infiltration of CD11b-positive inflammatory cells (for example, monocytes/ macrophages, and possibly myeloid-derived suppressor cells) was significantly decreased after EP treatment and/or RAGE knockdown (Figure 5d), suggesting that HMGB1/RAGE can influence the tumor microenvironment. We also observed that wild-type tumors expressing RAGE, when implanted into RAGE $^{-/-}$ mice, have significantly decreased tumor growth and about 30–40% less ATP production when compared with those implanted in wild-type mice (Figures 5e and f). This suggests that non-tumor cells within the tumor microenvironment have critical roles within the HMGB1/RAGE signaling system.

## DISCUSSION

We previously reported that HMGB1 is a critical regulator of apoptosis and autophagy in response to metabolic and therapeutic stress.[20,25–28] We hypothesized that the role of HMGB1 in pancreatic tumor survival might involve alterations in tumor bioenergetics. We indeed observed that recombinant HMGB1 or endogenous HMGB1 in necrotic tumor cell lysates increased ATP levels in both human and murine tumor cell lines. Although HMGB1 has been classically linked to increased inflammation, our studies have now linked it to alterations in tumor metabolism. Although HMGB1 is generally expressed at high levels in all nucleated cells, we observed increased expression of HMGB1 in human pancreatic tumor tissue when compared with nontransformed adjacent tissues, suggesting that tumors may also utilize this function of HMGB1 to promote progression.

HMGB1 interacts with several cell surface receptors, including RAGE, the toll-like receptors-4 (TLR-4) and −2 (TLR-2), and CD24/ Siglec 10, the latter serving as a negative signaling molecule, limiting inflammation.[29] Our findings suggest that RAGE is the major receptor responsible for the HMGB1-mediated effects on ATP production (Figure 6). RAGE consists of three extracellular immunoglobulin-like domains, a single transmembrane domain and a cytosolic domain. Antibodies neutralizing RAGE and targeted knockdown full-length RAGE inhibit HMGB1-mediated ATP production. It is interesting to note that the targeted knockdown of RAGE leads to a decrease in basal ATP levels and mitochondrial respiration, but neutralizing antibodies do not. This suggests that constitutive expression of intracellular RAGE is necessary to support optimal ATP production in the steady state. Ex-RAGE is important, but not essential for extracellular HMGB1-mediated ATP production. In contrast, cyt-RAGE is sufficient to drive HMGB1-induced ATP production. A recent study indicates that endocytosis pathways directly mediate extracellular HMGB1 uptake into cells.[16] We found that the caveolin inhibitor indomethacin inhibited HMGB1-mediated ATP production when cyt-RAGE was overexpressed in RAGE knockdown cells, suggesting that the caveolin-dependent endocytosis pathway mediated HMGB1-induced activation of cyt-RAGE in the absence of ex-RAGE (Figure 6).

The identification of the precise molecular signaling pathways by which RAGE signals, has been a topic of substantial inquiry and investigation. RAGE is present in the immune precipitates of mitochondrial extracts, where the immune precipitates of complex I and II contain RAGE. In addition, recent studies also found that HMGB1 can be located to mitochondria,[20,30] suggesting the HMGB1–RAGE pathway's special role in mitochondria. It remains unclear exactly to which protein RAGE binds, and whether RAGE recognizes already bound HMGB1. In pancreatic tumor cell lines, we found that exogenous HMGB1 induced phosphorylation of RAGE at Ser377, and its association with p-ERK1/2 as critical

steps in the regulation of mitRAGE location and tumor cell metabolism. Recent studies suggest that p-ERK1/2 in the outer membrane and intermembrane space is a crucial mitochondrial kinase to regulate molecular transport and mitochondrial respiration.[31–34] We demonstrate that there is a direct interaction between RAGE and p-ERK1/2, and ERK inhibitors and MEK2 siRNA inhibit HMGB1-induced p-RAGE and mitRAGE. Numerous RAGE protein isoforms are detectable in tissues and cell lines,[35] supporting the possible presence of RAGE in different organelles by post-translational modification and proteolytic cleavages. Production of sRAGE through transmembrane cleavage by ADAM-10 of the cell surface protein has been described,[31] although the mitRAGE expressed appears to be full length, and we favor directed transport of newly synthesized RAGE. We found that mutating the mitochondrial localization signal (Ser377A mutant), or a dominant negative mutant that retains surface and transmembrane RAGE (exm-RAGE) impaired the localization of mitRAGE and subsequent ATP production. These findings suggest that ERK1/2-mediated phosphorylation of RAGE at Ser377 regulates its mitochondrial location.

$RAGE^{-/-}$ mice are resistant to 9, 10-dimethylbenz [a] anthracene/12-O-tetradecanoylphorbol-13-acetate (TPA)-induced skin carcinogenesis[36] and mutant *KRAS*-induced pancreatic tumorigenesis.[9,37] Targeted inhibition of the HMGB1/RAGE pathway *in vivo* impairs pancreatic tumor growth that is associated with decreased tumor ATP levels and inflammation.

It has been appreciated for some time that alterations in metabolism are critical to allow for a selective growth advantage of transformed cells and cancer progression. A growing body of literature has focused on the ability of common oncogenes to alter metabolic pathways (specifically glycolysis). The hypothesis is that acquired mutations in these oncogenes, over time, confer a selective growth advantage to the tumor cell.[1,3] We propose a provocative new model in which inflammatory signals within the tumor microenvironment might also promote favorable tumor bioenergetics supporting tumor progression. In the setting of cancer, frequently associated with hypoxia, it may also be released during nutrient deprivation, oncogenic stress or other circumstances associated with enhanced autophagy, an important regulator of cellular metabolism.[38] In the setting of cancer, HMGB1 promotes RAGE translocation to mitochondria, leading to enhanced complex I activity and increased ATP production. Key steps in the bioenergetic pathways that can be influenced by signaling pathways include PI3K/PTEN/AKT, LKB1/ AMPK and STAT3.[39] We have also demonstrated that RAGE-mediated autophagy is required for IL-6-induced mitochondrial translocation of STAT3 and subsequently, IL-6/STAT3-mediated ATP production.[40] However, IL-6 cannot induce mitochondrial translocation of RAGE. These studies suggest that there are at least two different mechanisms involved in RAGE-mediated ATP production: mitRAGE dependent and RAGE-mediated autophagy dependent. It would be interesting to identify the genes and mechanisms that mediate the crosstalk between these two pathways.

In summary, we observe that HMGB1 stimulates pancreatic tumor cell proliferation and ATP production. Through cell fractionation experiments and confocal microscopy, we demonstrate that a proportion of RAGE is present in the mitochondria, where it associates with complex I and II. HMGB1 increases the levels of RAGE in the mitochondria, and tumors show increased RAGE expression relative to normal tissues. HMGB1 induces RAGE serine phosphorylation (through MEK2/ERK), and S377 is critical for mitochondrial location of RAGE and ATP production. Inhibition of HMGB1 or RAGE reduces tumor growth. These findings support clinical development of agents that target HMGB1 or RAGE for the treatment of human adenocarcinoma of the pancreas and likely many other epithelial neoplasms.

## MATERIALS AND METHODS

### Reagents

The antibodies to PARP, green-fluorescent protein (GFP), Bcl-2, ERK, p-ERK (Thr202/Tyr204), histone H3, p-p65, mitochondrial cytochrome oxidase IV and Pan-cadherin were obtained from Cell Signaling Technology (Danvers, MA, USA). The antibodies to tubulin and actin were obtained from Sigma (St Louis, MO, USA). The antibodies to TLR-2, TLR-4, phosphoserine and mitHSP70 were obtained from Abcam (Cambridge, MA, USA). The antibodies to HMGB1, microtubule-associated protein light chain 3 (LC3)-I/II, and calnexin were obtained from Novus (Littleton, CO, USA). The antibodies to the RAGE were obtained from Sigma, Abcam or RD Systems (Minneapolis, MN, USA). Anti-CD11b antibody was obtained from BD Biosciences (San Jose, CA, USA). The antibodies to IL-1β and IFN-γ were obtained from RD Systems. The antibodies to CD24, MEK-2 and p65 came from Santa Cruz Technology (Santa Cruz, CA, USA); complex I–IV immunocapture and the antibodies to the complex I subunit NDUFA9, complex II subunit 70 kDa Fp, complex III subunit Core 2, complex IV subunit 1 and retinoid IFN induced mortality (GRIM)-19 protein were obtained from Mitosciences (Eugene, OR, USA). Recombinant HMGB1 proteins were generously provided by the Eli Lilly Company (Indianapolis, IN, USA), with endotoxin content ≤3.1 EU/ml. The Mem–PER Eukaryotic Membrane Protein Extraction Kit came from ThermoFisher Scientific (Rockford, IL, USA). All other reagents were obtained from Sigma.

### Tumor cell lines and tumor tissue

Pancreatic tumor cell lines (human Panc2.03, human Panc3.27, mouse Panc02) were purchased from the American Type Culture Collection (Manassas, VA, USA) or the National Institutes of Health (Bethesda, MD, USA). Wild-type and HMGB1 $^{-/-}$ immortalized MEFs were a kind gift from Dr Marco E. Bianchi (San Raffaele Institute,Milan, Italy).[8] All cell lines were cultured in RPMI 1640 or DMEM medium supplemented with 10% heat-inactivated fetal bovine serum, 2 mM glutamine and antibiotic–antimycotic mix in a humidified incubator with 5% $CO_2$ and 95% air. Necrotic cells and apoptotic cells were prepared as previously described.[10] Pancreatic tumor tissue was collected under University of Pittsburgh approved protocol no. 21068. Tissue was harvested immediately following resection, and snap frozen at − 80 °C. Several representative hematoxylin and eosin slides were obtained at the time of collection, and evaluated by a pathologist to identify tissues as tumor or adjacent control pancreas.

### RAGE plasmid construction and transfection

The coding sequence of the mouse full length and various domains of RAGE protein was expanded by PCR from an expression vector containing the mouse RAGE (pUNO1-m-RAGE) open reading frame obtained from Invitrogen (San Diego, CA, USA), using the following primers containing *Eco*RI and *Xba*I restriction sites at their 5’ and 3’ ends, respectively: full-length RAGE (1–403), forward 5′-CAATGAATTCATGCCAGCGGGGAC AGCAGC-3′ and reverse 5′-AATTTCTAGATACGGTCCCCCGGCACCATTC-3′; Ex-RAGE (1–341), forward 5′-CAATGAATTCATGCCAGCGGGGACAGCAGC-3′ and reverse 5′-TACATCTAGAGCTAGCGTACCCAGCCCAGACT-3′; m-RAGE (342–362), forward 5′-CAGTGAATTCATGGCCCTGGCCTTGGGGATCCT-3′, reverse 5′-AAATTCTAGACACAGGATAGCCCCGACGAGCA-3′; Cyt-RAGE (363–403), forward 5′-CCAGGAATTCATGTGGCGAAAACGACAACCCAG-3′ and reverse 5′-AATTTCTAGATACGGTCCCCCGGCACCATTC-3′; Exm-RAGE (1–362), forward 5′-CAATGAATTCATGCCAGCGGGGACAGCAGC-3′, reverse 5′-AAATTCTAGACACAGGATAGCCCCGACGAGCA-3′. The RAGE cDNA sequences

generated by PCR were subcloned into the vector pAcGFP-C2 (Clonetech, Mountain View, CA, USA). All plasmids were sequence-verified by the University of Pittsburgh sequencing facility.

Using a site-directed mutagenesis kit (Stratagene, La Jolla, CA, USA), a point mutation was created mutating Ser377 to Ala377 and/or Ser399 to Ala399 in RAGE in the pAcGFP-C2-RAGE plasmid using the following primers: 5′-GGAAGGCCCCGGAAGCCCAGGAGGATGAGGAG-3′ (S377A forward primer); 5′-CTCCTCATCCTCCTGGGCTTCCGGGGCCTTCC-3′ (S377A reverse primer); 5′-GCAGAGCTGAATCAGGCCGAGGAAGCGGAGATG-3′ (S399A forward primer); 5′-CATCTCCGCTTCCTCGGCCTGATTCAGCTCTGC-3′ (S399A reverse primer). All plasmid mutants were sequence-verified.

Empty vector, vectors encoding wild-type RAGE, and individual mutants of RAGE were transfected into Panc02 cells using the FuGENE transfection reagent (Roche Applied Science, Stockholm, Sweden). Stable clones were obtained with G418 (400 μg/ml) selection for 2–3 weeks.

## Isolation and subcellular fractionation of mitochondria

Subcellular fractionation of pancreatic tissue and pancreatic tumor cells was carried out with mitochondria isolation kits obtained from Pierce (Rockford, IL, USA). Cells were harvested by centrifuging at 850 *g* for 2 min. The pellet was suspended with 800 μl of Reagent A and then incubated for exactly 2 min on ice, according to the manufacturer's instructions. Next, 10 μl of Reagent B was added to the suspended solution and incubated for 5 min on ice with vortexing at maximum speed every minute. For tissues, 50–200 mg of tissue was washed twice with 2–4 ml of phosphate buffered saline (PBS). After carefully removing and discarding the PBS wash, the tissue was cut into small pieces and 800 μl of bovine serum albumin/ Reagent A solution was added. Dounce homogenization was performed on ice, and 800 μl of Reagent C was then added to the solution and the tube was inverted several times to mix. The solution was centrifuged at 700 *g* for 10 min at 4°C, and the pellet was used for the crude nuclei fraction. The supernatant was continuously centrifuged at 3000 *g* for 15 min at 4°C and transferred to a new tube to obtain the post-mitochondrial supernatant fraction. The pellet was washed with 500 μl of Reagent C and centrifuged at 1 2000 *g* for 5 min, then used for isolation of the mitochondrial fraction. To confirm that these were the appropriate fractions, the western blots were probed for cytochrome c oxidase IV as a mitochondrial marker, tubulin as a cytoplasmic marker, calnexin as an endoplasmic reticulum marker and histone H3 as a nuclear marker. In most experiments, we detected little or no tubulin or calnexin in the mitochondrial fraction.

## Subcutaneous tumor models

To generate murine subcutaneous tumors, $10^6$ normal Panc02 cells or cells stably transfected with control or RAGE-specific shRNA were injected subcutaneously to the right of the dorsal midline in wild-type or $RAGE^{-/-}$ mice (The Jackson Laboratory, Bar Harbor, Maine, USA, and a kind gift from Angelika Bierhaus, Heidelberg, respectively) as previously described.[7] Both wild-type and $RAGE^{-/-}$ mice were on a C57BL/6 background,[41] and were housed in conventional caging in a pathogen-free and under negative-pressure conditions. Tumors were measured twice weekly, and volumes were calculated using the formula length $\times$ width$^2$ $\times$ $\pi/6$. The procedures for performing animal experiments were approved, and in accordance with the principles and guidelines of the University of Pittsburgh Institutional Animal Care and Use Committee.

### Western blotting

Proteins in the cell lysate were resolved on 4–12% Criterion XT Bis-Tris gels (Bio-Rad, Hercules, CA, USA) and transferred to a nitrocellulose membrane as previously described.[6,7] After blocking, the membrane was incubated for 2h at 25 °C or overnight at 4°C with various primary antibodies. After incubation with peroxidase-conjugated secondary antibodies for 1 h at 25 °C, the signals were visualized by enhanced chemiluminescence (Pierce) according to the manufacturer's instructions. The relative band intensity was quantified using the Gel-pro Analyzer software (Media Cybernetics, Bethesda, MD, USA).

### RNA interference

RAGE-short hairpin RNA (shRNA), TLR2-shRNA, TLR4-shRNA, CD24-shRNA, p65-shRNA and control-shRNA were obtained from Sigma, and transfected into cells using the Lipofectamine 2000 reagent (Life Technologies, Carlsbad, CA, USA) according to the manufacturer's instructions. To generate stable shRNA expressing lines, positive cells were selected with 1–2 μg/ml puromycin for 2–3 weeks. MEK2-small interfering RNA (siRNA) and control-siRNA from Santa Cruz Technology were transfected into cells using X-tremeGENE siRNA reagent (Roche Applied Science) according to the manufacturer's instructions.

### Immunofluorescence analysis

Cells were cultured on glass coverslips and fixed in 3% formaldehyde for 30 min at room temperature prior to detergent extraction with 0.1% Triton X-100 for 10 min at 25 °C. Coverslips were saturated with 2% bovine serum albumin in PBS for 1 h at room temperature, and processed for immunofluorescence with primary antibodies followed by Alexa Fluor 488 or Cy3-conjugated IgG (Invitrogen), respectively. Nuclear morphology was analyzed with the fluorescent dye Hoechst 33342 (Invitroge). Between all incubation steps, cells were washed three times for 3 min with 0.5% bovine serum albumin in PBS. Images were taken with an Olympus Fluoview 1000 confocal microscope (Olympus Corp, Tokyo, Japan), and fluorescence signals were measured by Image-Pro Plus platform (Media Cybernetics).

For tissue immunofluorescence analysis, tissues were embedded in an optimum cutting temperature cryomedium (Sakura, Zoeterwoude, the Netherlands) and subsequently, cut into 8 μm sections as previously described.[2] Tissue sections were stained with HMGB1, RAGE or CD11b antibody followed by Alexa Fluor 488- or Cy3-conjugated IgG, respectively. Nuclear morphology was analyzed with the fluorescent dye Hoechst 33342. Mitochondria were imaged following staining with a complex I antibody (Mitosciences).

### Immunoprecipitation analysis

Cells were lysed at 4 °C in ice-cold modified radioimmunoprecipitation lysis buffer (Millipore, Billerica, MA, USA), and cell lysates were cleared by centrifugation (12000 *g*, 10 min). Concentrations of proteins in the supernatant were determined by bicinchoninic acid assay. Prior to immunoprecipitation, samples containing equal amount of proteins were pre-cleared with Protein A or Protein G agarose/sepharose (Millipore) (4°C, 3 h), and subsequently incubated with various irrelevant IgG or specific antibodies (2–5 μg/ml) in the presence of Protein A or G agarose/sepharose beads for 2 h or overnight at 4 °C with gentle shaking. Following incubation, agarose/ sepharose beads were washed extensively with PBS, and proteins were eluted by boiling in 2 × sodium dodecyl sulfate (SDS) sample buffer before SDS–PAGE electrophoresis. To detect phosphorylation of RAGE and complex I, cell

extracts were immunoprecipitated with anti-RAGE antibody or immunocapture antibody, respectively, and analyzed with anti-phosphoserine antibody by western blotting.

### ATP assay

The ATP content in whole cell or tissue extracts was determined with a luminescent ATP detection kit (ATPlite, PerkinElmer Life Sciences, Boston, MA, USA) according to the manufacturer's instructions. The luminescent intensity was measured using a microplate reader (Synergy 2, BioTek instruments, Winooski, VT, USA). In parallel, cell number in whole cell samples and protein concentration in the tissue extracts were conventionally determined by trypan blue exclusion or bicinchoninic acid assay, respectively. The results in cells are expressed as relative ATP level compared to controls after normalizing for cell number. The results in tissues are expressed as relative ATP level compared to controls after normalizing for protein concentration.

### Complex I enzyme activity assay

The activity of complex I was determined with a Complex I Enzyme Activity Assay Kit (Mitosciences), according to the manufacturer's instructions.

### NF- κB activation assay

Cells were transiently transfected in a 12-well plate with NF- κB luciferase reporter plasmid and control empty plasmid using lipofectamine 2000 reagent (Life Technologies), according to the manufacturer's instructions. After 24–48 h, the cells were exposed to various agents. The luciferase activity was determined using the luciferase assay system with the reporter lysis buffer obtained from Promega (Madison, WI, USA), as previously described.[42] The results are expressed as relative NF- κB activity after normalizing for the control empty plasmid.

### Transwell migration assay

Transmigration of pancreatic tumor cells was performed as previously described.[43,44] Described briefly, 0.47cm$^2$ transwells (Nunc, Rochester, NY, USA) with polycarbonate membranes (8 μm pore size) were coated with gelatin (Sigma) for 1 h at 37 °C. Cells ($5 \times 10^4$) were seeded on top of transwell filters in RPMI containing 2% fetal bovine serum and allowed to migrate towards RPMI containing 10% fetal bovine serum in the absence or presence of HMGB1/Rote in the lower compartment of the transwell system for 20–24 h. The number of cells that migrated was estimated by trypan blue staining.

### OXPHOS and glycolysis assays

Cellular OXPHOS and glycolysis were monitored using the Seahorse Bioscience Extracellular Flux Analyzer (XF24, Seahorse Bioscience Inc., North Billerica, MA, USA) by measuring the OCR, indicative of respiration and ECR, indicative of glycolysis in real time as previously described.[20] Described briefly, 30 000–50 000 cells were seeded in 24-well plates designed for XF24 in 150 μl of appropriate growth media and incubated overnight. Prior to performing measurements, cells were washed once with unbuffered media, then immersed in 675 μl unbuffered media and incubated in the absence of $CO_2$ for 1 h. The OCR and ECR were then measured in a typical 8-min cycle of mix (2–4 min), dwell (2 min) and measure (2–4 min) as recommended by Seahorse Bioscience. The basal levels of OCR and ECR were recorded first, followed by the OCR and ECR levels following injection of compounds that inhibit the respiratory mitochondrial electron transport chain, ATP synthesis or glycolysis. Each reading under specific conditions was repeated at least three times.

### Statistical analysis

Data are expressed as means±s.d. of two or three independent experiments performed in triplicate. One-way ANOVA was used for comparison among the different groups. When the ANOVA was significant, post hoc testing of differences between groups was performed using Fisher's least significant difference test. Otherwise, Student's *t*-test was used for comparison of the means of two groups. A *P*-value <.05 was considered significant.

## Supplementary Material

Refer to Web version on PubMed Central for supplementary material.

## Acknowledgments

We dedicate this manuscript to the memory of Angelika Bierhaus, PhD, our friend and benefactor. She was a pioneering RAGE biologist, generous and kind in her dealings with colleagues, who provided us the mice with which we completed this work, and who sadly passed away on 15 April 2012 after a long and courageous battle with cancer. Angelika had a great love of life and she was generous, kind and warm hearted. She was always full of plans for scientific endeavors, even when her disease began to take its toll. She steadfastly denied that she would be defeated, recently celebrating her 50th birthday; however, she was aware that her remaining time was short. She dedicated herself to research, but despite her incredible strength, she was not able to overcome the disease, which tragically took her life.We thank Christine Heiner (University of Pittsburgh. Department of Surgery) for her critical reading of the manuscript. This project was supported by grants from the National Institutes of Health (P01 CA 101944 to MTL, R01CA160417 to DT) and the University of Pittsburgh (DT and HJZ). This project used University of Pittsburgh Cancer Institute shared resources that are supported in part by award P30CA047904. We also thank Dr Donna Stolz and Simon Watkins for providing the confocal microscopy facilities at the Center for Biologic Imaging at University of Pittsburgh School of Medicine.

## REFERENCES

1. Hanahan D, Weinberg RA. Hallmarks of cancer: the next generation. Cell. 2011; 144:646–674. [PubMed: 21376230]
2. Vakkila J, Lotze MT. Inflammation and necrosis promote tumour growth. Nat Rev Immunol. 2004; 4:641–648. [PubMed: 15286730]
3. Vander Heiden MG, Cantley LC, Thompson CB. Understanding the Warburg effect: the metabolic requirements of cell proliferation. Science. 2009; 324:1029–1033. [PubMed: 19460998]
4. Tang D, Kang R, Zeh HJ 3rd, Lotze MT. High-mobility group box 1 and cancer. Biochim Biophys Acta. 2010; 1799:131–140. [PubMed: 20123075]
5. Lotze MT, Tracey KJ. High-mobility group box 1 protein (HMGB1): nuclear weapon in the immune arsenal. Nat Rev Immunol. 2005; 5:331–342. [PubMed: 15803152]
6. Kang R, Tang D, Livesey KM, Schapiro NE, Lotze MT, Zeh HJ 3rd. The receptor for advanced glycation end-products (RAGE) protects pancreatic tumor cells against oxidative injury. Antioxid Redox Signal. 2011; 15:2175–2184. [PubMed: 21126167]
7. Kang R, Tang D, Schapiro NE, Livesey KM, Farkas A, Loughran P, et al. The receptor for advanced glycation end products (RAGE) sustains autophagy and limits apoptosis, promoting pancreatic tumor cell survival. Cell Death Differ. 2010; 17:666–676. [PubMed: 19834494]
8. Calogero S, Grassi F, Aguzzi A, Voigtlander T, Ferrier P, Ferrari S, et al. The lack of chromosomal protein Hmg1 does not disrupt cell growth but causes lethal hypoglycaemia in newborn mice. Nat Genet. 1999; 22:276–280. [PubMed: 10391216]
9. Kang R, Louxa T, Tang D, Schapiroa NE, Vernona P, Liveseya KM, et al. RAGE expression is permissive for early pancreatic neoplasia. Proc Natl Acad Sci USA. 2012
10. Scaffidi P, Misteli T, Bianchi ME. Release of chromatin protein HMGB1 by necrotic cells triggers inflammation. Nature. 2002; 418:191–195. [PubMed: 12110890]
11. Bianchi ME. HMGB1 loves company. J Leukoc Biol. 2009; 86:573–576. [PubMed: 19414536]
12. Mantovani A. Cancer: inflaming metastasis. Nature. 2009; 457:36–37. [PubMed: 19122629]

13. Palumbo R, Sampaolesi M, De Marchis F, Tonlorenzi R, Colombetti S, Mondino A, et al. Extracellular HMGB1, a signal of tissue damage, induces mesoangioblast migration and proliferation. J Cell Biol. 2004; 164:441–449. [PubMed: 14744997]
14. Rai V, Maldonado AY, Burz DS, Reverdatto S, Schmidt AM, Shekhtman A. Signal transduction in receptor for advanced glycation end products (RAGE): solution structure of C-terminal rage (ctRAGE) and its binding to mDia1. J Biol Chem. 2012; 287:5133–5144. [PubMed: 22194616]
15. Hudson BI, Kalea AZ, Del Mar Arriero M, Harja E, Boulanger E, D'Agati V, et al. Interaction of the RAGE cytoplasmic domain with diaphanous-1 is required for ligand-stimulated cellular migration through activation of Rac1 and Cdc42. J Biol Chem. 2008; 283:34457–34468. [PubMed: 18922799]
16. Zhang Y, Li W, Zhu S, Jundoria A, Li J, Yang H, et al. Tanshinone IIA sodium sulfonate facilitates endocytic HMGB1 uptake. Biochem Pharmacol. 2012; 84:1492–1500. [PubMed: 23022229]
17. Schmidt AM, Yan SD, Yan SF, Stern DM. The multiligand receptor RAGE as a progression factor amplifying immune and inflammatory responses. J Clin Invest. 2001; 108:949–955. [PubMed: 11581294]
18. Sparvero LJ, Asafu-Adjei D, Kang R, Tang D, Amin N, Im J, et al. RAGE (receptor for advanced glycation endproducts), RAGE ligands, and their role in cancer and inflammation. J Transl Med. 2009; 7:17. [PubMed: 19292913]
19. Wegrzyn J, Potla R, Chwae YJ, Sepuri NB, Zhang Q, Koeck T, et al. Function of mitochondrial Stat3 in cellular respiration. Science. 2009; 323:793–797. [PubMed: 19131594]
20. Tang D, Kang R, Livesey KM, Kroemer G, Billiar TR, Van Houten B, et al. High-mobility group box 1 is essential for mitochondrial quality control. Cell Metab. 2011; 13:701–711. [PubMed: 21641551]
21. Pagliarini DJ, Dixon JE. Mitochondrial modulation: reversible phosphorylation takes center stage? Trends Biochem Sci. 2006; 31:26–34. [PubMed: 16337125]
22. Mitola S, Belleri M, Urbinati C, Coltrini D, Sparatore B, Pedrazzi M, et al. Cutting edge: extracellular high mobility group box-1 protein is a proangiogenic cytokine. J Immunol. 2006; 176:12–15. [PubMed: 16365390]
23. Tang D, Kang R, Xiao W, Wang H, Calderwood SK, Xiao X. The anti-inflammatory effects of heat shock protein 72 involve inhibition of high-mobility-group box 1 release and proinflammatory function in macrophages. J Immunol. 2007; 179:1236–1244. [PubMed: 17617616]
24. Ulloa L, Ochani M, Yang H, Tanovic M, Halperin D, Yang R, et al. Ethyl pyruvate prevents lethality in mice with established lethal sepsis and systemic inflammation. Proc Natl Acad Sci USA. 2002; 99:12351–12356. [PubMed: 12209006]
25. Huang J, Ni J, Liu K, Yu Y, Xie M, Kang R, et al. HMGB1 promotes drug resistance in osteosarcoma. Cancer Res. 2012; 72:230–238. [PubMed: 22102692]
26. Livesey K, Kang R, Vernon P, Buchser W, Loughran P, Watkins SC, et al. p53/HMGB1 complexes regulate autophagy and apoptosis. Cancer Res. 2012; 72:1996–2005. [PubMed: 22345153]
27. Tang D, Kang R, Livesey KM, Cheh CW, Farkas A, Loughran P, et al. Endogenous HMGB1 regulates autophagy. J Cell Biol. 2010; 190:881–892. [PubMed: 20819940]
28. Tang D, Kang R, Cheh CW, Livesey KM, Liang X, Schapiro NE, et al. HMGB1 release and redox regulates autophagy and apoptosis in cancer cells. Oncogene. 2010; 29:5299–5310. [PubMed: 20622903]
29. Andersson U, Tracey KJ. HMGB1 is a therapeutic target for sterile inflammation and infection. Annu Rev Immunol. 2011; 29:139–162. [PubMed: 21219181]
30. Stumbo AC, Cortez E, Rodrigues CA, Henriques MG, Porto LC, Barbosa HS, et al. Mitochondrial localization of non-histone protein HMGB1 during human endothelial cell-Toxoplasma gondii infection. Cell Biol Int. 2008; 32:235–238. [PubMed: 17936030]
31. Poderoso C, Converso DP, Maloberti P, Duarte A, Neuman I, Galli S, et al. A mitochondrial kinase complex is essential to mediate an ERK1/2-dependent phosphorylation of a key regulatory protein in steroid biosynthesis. PLoS ONE. 2008; 3:e1443. [PubMed: 18197253]

32. Alonso M, Melani M, Converso D, Jaitovich A, Paz C, Carreras MC, et al. Mitochondrial extracellular signal-regulated kinases 1/2 (ERK1/2) are modulated during brain development. J Neurochem. 2004; 89:248–256. [PubMed: 15030409]
33. Antico, Arciuch VG.; Alippe, Y.; Carreras, MC.; Poderoso, JJ. Mitochondrial kinases in cell signaling: facts and perspectives. Adv Drug Deliv Rev. 2009; 61:1234–1249. [PubMed: 19733603]
34. Galli S, Jahn O, Hitt R, Hesse D, Opitz L, Plessmann U, et al. A new paradigm for MAPK: structural interactions of hERK1 with mitochondria in HeLa cells. PLoS ONE. 2009; 4:e7541. [PubMed: 19847302]
35. Gefter JV, Shaufl AL, Fink MP, Delude RL. Comparison of distinct protein isoforms of the receptor for advanced glycation end-products expressed in murine tissues and cell lines. Cell Tissue Res. 2009; 337:79–89. [PubMed: 19415334]
36. Gebhardt C, Riehl A, Durchdewald M, Nemeth J, Furstenberger G, Muller-Decker K, et al. RAGE signaling sustains inflammation and promotes tumor development. J Exp Med. 2008; 205:275–285. [PubMed: 18208974]
37. DiNorcia J, Lee MK, Moroziewicz DN, Winner M, Suman P, Bao F, et al. RAGE gene deletion inhibits the development and progression of ductal neoplasia and prolongs survival in a murine model of pancreatic cancer. J Gastrointest Surg. 2012; 16:104–112. discussion 112. [PubMed: 22052106]
38. Rabinowitz JD, White E. Autophagy and metabolism. Science. 2010; 330:1344–1348. [PubMed: 21127245]
39. Hsu PP, Sabatini DM. Cancer cell metabolism: Warburg and beyond. Cell. 2008; 134:703–707. [PubMed: 18775299]
40. Kang R, Loux T, Tang D, Schapiro NE, Vernon P, Livesey KM, et al. The expression of the receptor for advanced glycation endproducts (RAGE) is permissive for early pancreatic neoplasia. Proc Natl Acad Sci USA. 2012; 109:7031–7036. [PubMed: 22509024]
41. Liliensiek B, Weigand MA, Bierhaus A, Nicklas W, Kasper M, Hofer S, et al. Receptor for advanced glycation end products (RAGE) regulates sepsis but not the adaptive immune response. J Clin Invest. 2004; 113:1641–1650. [PubMed: 15173891]
42. Wang S, Kotamraju S, Konorev E, Kalivendi S, Joseph J, Kalyanaraman B. Activation of nuclear factor-kappaB during doxorubicin-induced apoptosis in endothelial cells and myocytes is pro-apoptotic: the role of hydrogen peroxide. Biochem J. 2002; 367:729–740. [PubMed: 12139490]
43. Orlova VV, Choi EY, Xie C, Chavakis E, Bierhaus A, Ihanus E, et al. A novel pathway of HMGB1-mediated inflammatory cell recruitment that requires Mac-1-integrin. Embo J. 2007; 26:1129–1139. [PubMed: 17268551]
44. Praus M, Wauterickx K, Collen D, Gerard RD. Reduction of tumor cell migration and metastasis by adenoviral gene transfer of plasminogen activator inhibitors. Gene Ther. 1999; 6:227–236. [PubMed: 10435107]

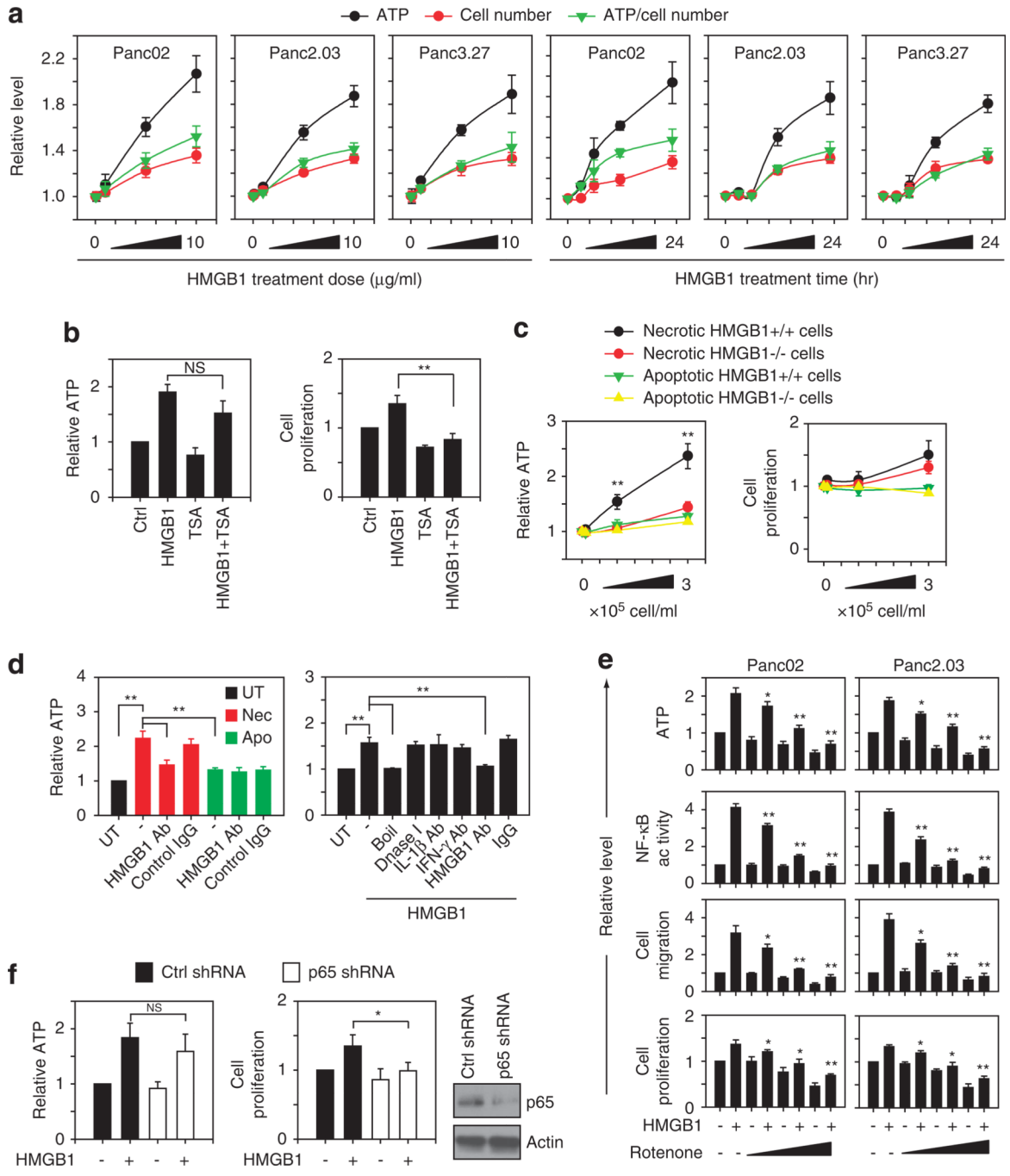


**Figure 1.**

HMGB1 promotes ATP production and subsequent cell growth, cell migration and NF-κB activation in pancreatic tumor cells. (**a**) Time course and dose-response effects of HMGB1 on ATP production and cell growth in cultured pancreatic tumor cell lines. The relative ATP level, with untreated control set as 1 (mean±s.d., $n = 3$), is shown. (**b**) Panc02 cells were treated with HMGB1 (10μg/ml) in the presence or absence of trichostatin A (400 nM), and then assayed for ATP levels and cellular proliferation. Data represent relative levels, with untreated control (ctrl) set as 1 (mean±s.d., $n = 3$, $^{**}P<0.001$, NS = not significant). (**c**) Lysed (necrotic) MEFs lacking HMGB1 do not elicit production of ATP at 24 h in Panc02

tumor cells. Data shown are the relative ATP levels, with the untreated ctrl set as 1 (mean ±s.d., $n = 3$, $^{**}P<0.001$). (**d**) Panc02 cells were treated with lysed $3 \times 10^5$ necrotic ('Nec') or apoptotic ('Apo') MEFs for 24 h in the presence or absence of HMGB1 Ab (50 μg/ml) or control IgG (left panel), and then assayed for ATP levels (right panel). Panc02 cells were treated with HMGB1 (10 μg/ml) for 24 h in the presence or absence of Dnase I (10 U/ml) and antibodies (50 μg/ml) as indicated, and then assayed for ATP levels (right panel). Relative ATP levels, with untreated ctrl set as 1 (mean±s.d., $n = 3$, $^{**}P<0.001$), are shown. (**e**) Pancreatic tumor cells were treated with HMGB1 (10 μg/ml) in the presence or absence of Rote (0.5, 1 and 2 μM), and then assayed for ATP levels, NF-κB activity by luciferase reporter assay, migration by transwell assay, and cell growth by counting cell number. Data represent relative level, with untreated ctrl set as 1 (mean±s.d., $n = 3$, $^{*}P<0.01$, $^{**}P<0.001$). (**f**) After transfection with p65 shRNA or ctrl shRNA for 48h, Panc02 cells were treated with HMGB1 (10 μg/ml) for 24 h and the ATP level was then analyzed. Data represent relative levels, with untreated ctrl shRNA set as 1 (mean±s.d., NS = not significant).

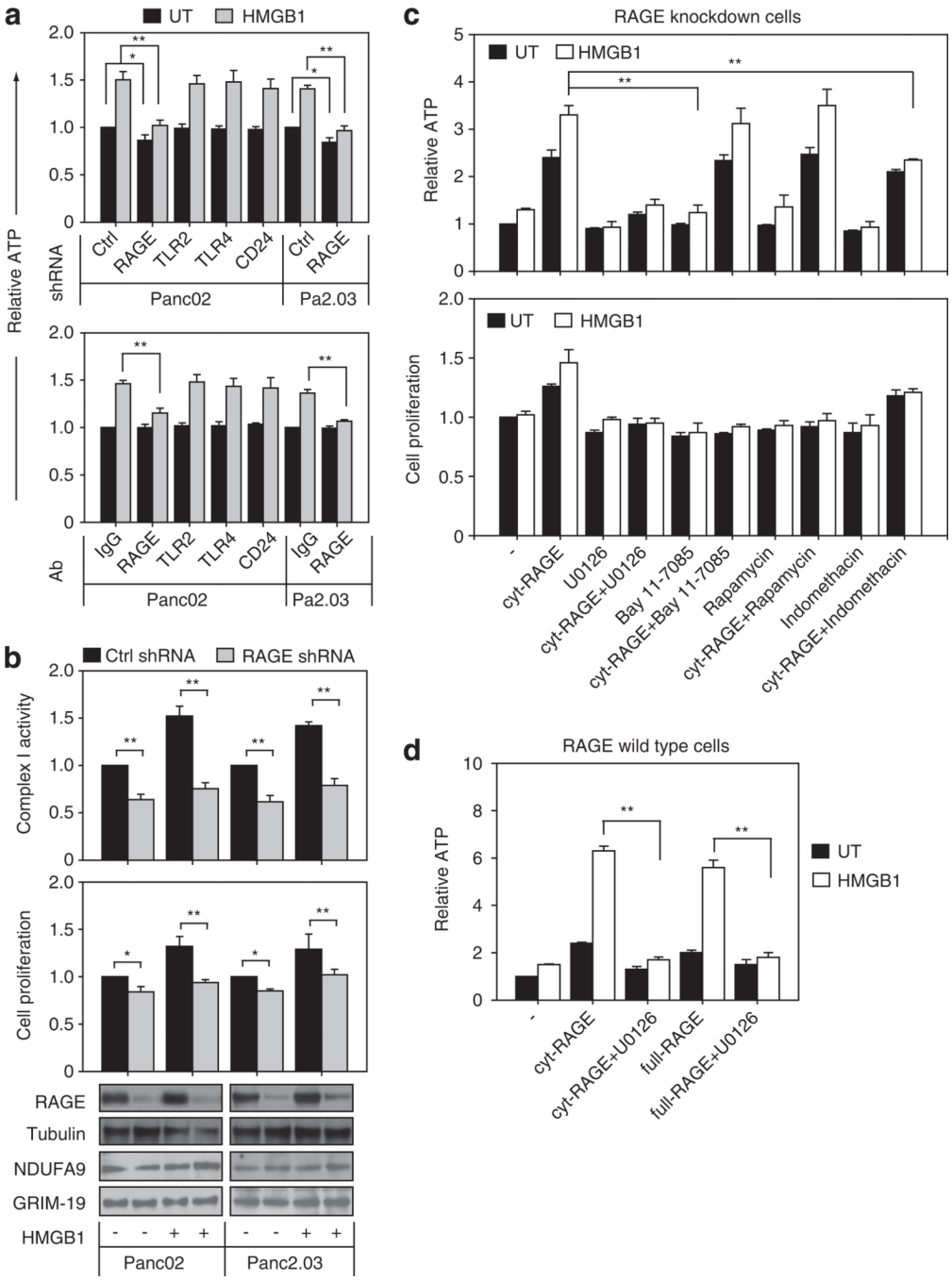


**Figure 2.**

RAGE is required for HMGB1-mediated ATP production. (**a**) Pancreatic tumor cells were transfected with specific shRNA (top panel) for 48 h or treated with the indicated antibody (Ab, 10 μg/ml, bottom panel) for 12 h, then treated with HMGB1 (10 μg/ml) for 24 h and assayed for ATP production. Data represent relative ATP levels, with untreated control set as 1 (mean±s.d., $n$= 3, *$P$ <0.05, **$P$ <0.001, NS: not significant). (**b**) RAGE knockdown inhibits mitochondrial complex I activity with or without HMGB1 (10 μg/ml) treatment for 24 h. Data represent relative levels of ATP and complex I activity, with untreated control shRNA set as 1 (mean±s.d., $n$ =3, **$P$ <0.001). (**c, d**) RAGE knockdown (**c**) or wild-type,

(**d**) Panc02 cells were transfected with ‘cyt-RAGE’ or full RAGE (‘full-RAGE’) as indicated, treated with or without U0126 (10 μM), Bay 11–7085 (10 μM), rapamycin (100 nM) and indomethacin (300 μM) for 1 h, and then treated with HMGB1 (10 μg/ml) for 24 h. Data represent relative levels of ATP and cellular proliferation, with untreated control set as 1 (mean±s.d., $n = 3$, $^{**}P < 0.001$).

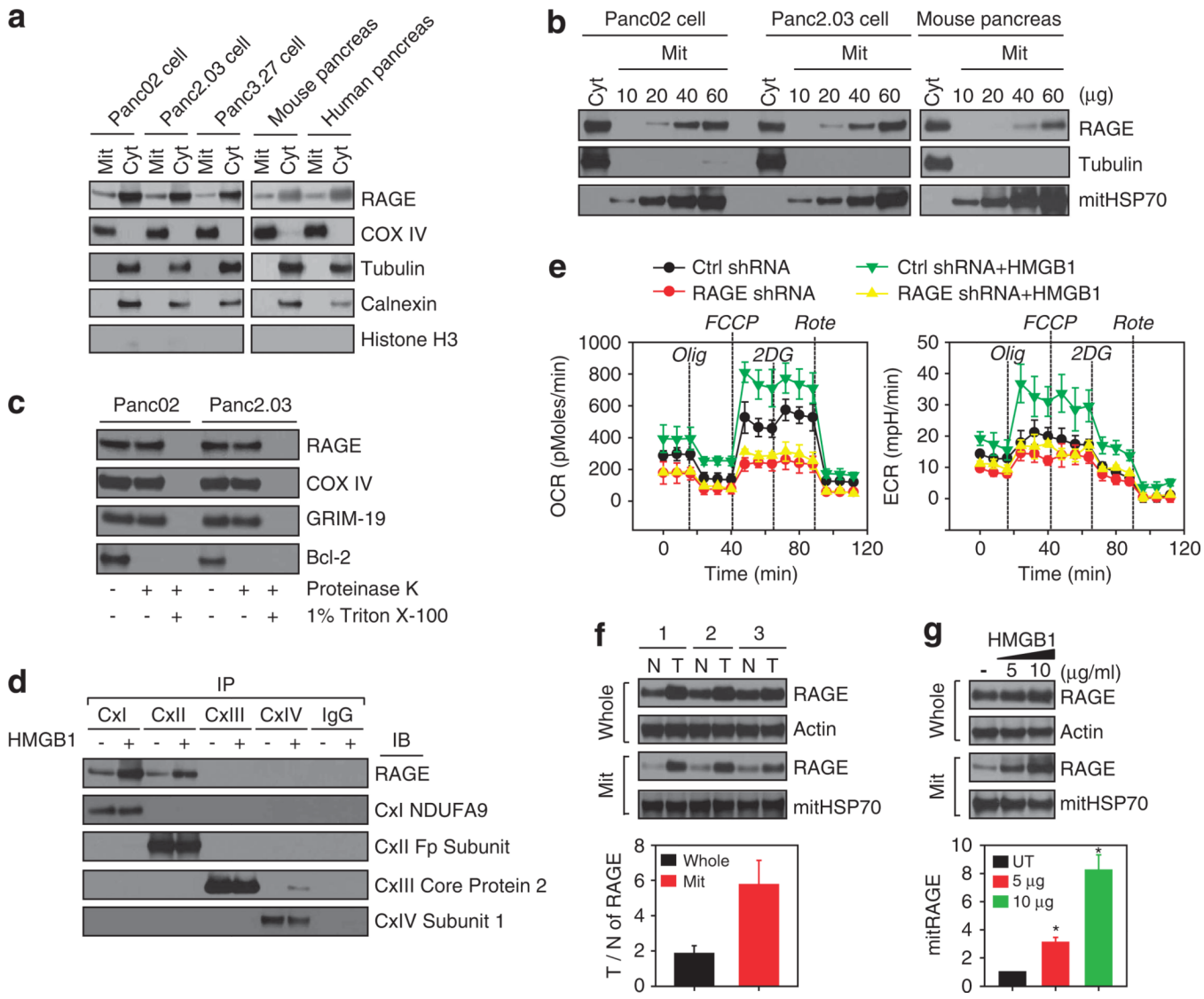


**Figure 3.**

HMGB1 treatment is associated with enhanced expression of RAGE in mitochondria. (**a**) Cytoplasmic (Cyto), and mitochondrial (Mit) was extracted from pancreatic tumor cells and pancreatic tissues were separated by SDS–PAGE. (**b**) Increasing amounts of mitochondrial extracts as indicated were probed for RAGE, tubulin and mitHSP70. (**c**) Mitochondria were isolated from pancreatic tumor cells and treated with 100 ng/ml of proteinase K for 15min in the absence or the presence of 1% Triton X-100. Samples were probed for RAGE, cytochrome oxidase IV, GRIM-19 and Bcl-2 by western blot. (**d**) Panc02 cells were treated with 10 μg/ml HMGB1 for 24 h, and antibodies to complex I–IV (CxI–IV) or a nonspecific control IgG were incubated with Panc02 mitochondrial extracts. Immunoprecipitates were resolved on SDS–PAGE and probed for RAGE, CxI NDUFA9, CxII Fp subunit, CxIII core protein 2 and CxIV subunit I by western blot. (**e**) RAGE knockdown (‘RAGE shRNA’) and wild-type (‘ctrl shRNA’) Panc02 cells were pretreated with 5μg/ml HMGB1 for 24 h, and then treated with oligomycin (1 uM), p-trifluoromethoxy carbonyl cyanide phenyl hydrazone (‘FCCP’, 0.3 uM), ‘2DG’, 100 mM, and Rote, 1 uM sequentially as indicated. OCR and ECR were monitored using the Seahorse Bioscience Extracellular Flux Analyzer in real time (mean±s.d., *n* =3). (**f**) Western blot analysis indicated protein in samples from whole or

mitochondrial extract from pancreatic tumor ('T') or nearby normal control ('N') tissues. Representative western blots (top panel) and quantifications of five patient tissues (bottom) are shown. (**g**) Panc02 cells were treated with 5–10 μg/ml HMGB1 for 24 h. Western blot analysis was then performed to detect RAGE, actin or mitHSP70 in whole cells or mitochondrial extracts. Relative mitRAGE (bottom panel) is shown as mean±s.d. ($n$=3 *$P$ <0.001 versus control).

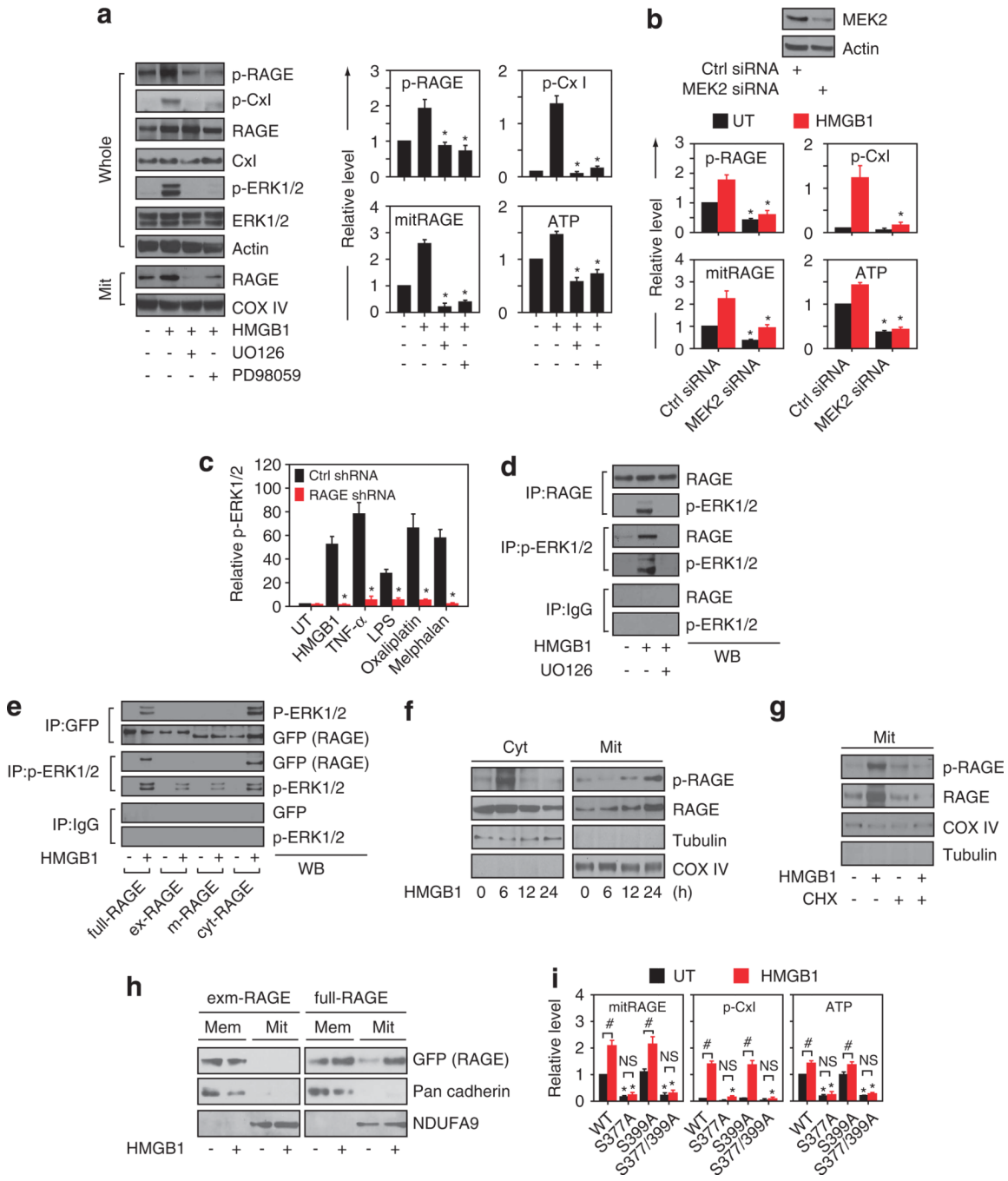


**Figure 4.**

Ser377 is required for RAGE activity in mitochondria. (**a**) Panc02 cells were treated with 10 μg/ml HMGB1 for 24 h in the absence or the presence of the ERK inhibitors U0126 and PD98059 (20 μM), followed by western blot analysis of whole cells or mitochondrial extracts. Quantitative data is shown in the right panel, with normal ctrl set as 1 or 0.1 (mean ±s.d., $n = 3$, $^*P < 0.001$ versus single HMGB1 group). (**b**) Knockdown of MEK2 by siRNA in Panc02 cells decreased relative levels of p-RAGE, p-CxI, mitRAGE, and ATP with or without 10 μg/ml HMGB1 treatment for 24 h. Data is shown as mean±s.d., with the normal control set as 1 or 0.1 ($n = 3$, $^*P < 0.001$ versus ctrl siRNA group). (**c**) uantitative analysis of

p-ERK in wild-type and RAGE knockdown Panc02 cells following treatment with a representative damage-associated molecular pattern molecule (HMGB1), pathogen-associated molecular pattern molecule (lipopolysaccharide), cytokine (TNFα) or chemotherapeutic drug (melphalan, oxaliplatin) as indicated for 24h (mean±s.d., $n$=3, *$P$ <0.001 versus ctrl shRNA group). (**d**) Antibodies to RAGE, p-ERK1/2 or a nonspecific control IgG were incubated with Panc02 extracts following 10 μg/ml HMGB1 treatment with or without U0126 (20 μm) for 12 h. Immunoprecipitates were resolved on SDS–PAGE and probed for RAGE, p-ERK1/2. (**e**) Panc02 cells were transfected with full-RAGE, ex-RAGE, m-RAGE and cyt-RAGE plasmids fused with a GFP-tag. Antibodies to GFP, p-ERK1/2 or a nonspecific control IgG were incubated with Panc02 extracts as indicated. Immunoprecipitates were resolved on SDS–PAGE and probed for GFP, p-ERK1/2. **(f)** Panc02 cells were treated with 10 μg/ml HMGB1 for 24 h, followed by western blot analysis of cytosolic (‘Cyt’) or mitochondrial (‘Mit’) extracts as indicated. (**G**) Panc02 cells 10 μg/ml HMGB1 for 24 h in the absence or the presence of cycloheximide (CHX, 10 μg/ml), followed by western blot analysis of mitochondrial extracts. (**h**) Panc02 cells were transfected with full-RAGE and exm-RAGE plasmids fused with a GFP-tag, then treated with 10 μg/ml HMGB1 for 24 h. western blot analysis of membrane (‘Mem’) and mitochondrial (‘Mit’) extracts. (**i**) Panc02 cells were transfected with full-RAGE (‘WT’) and mutants as indicated, and treated with 10 μg/ml HMGB1 for 24 h. Relative levels of mitRAGE, p-CxI, and ATP are shown as mean±s.d., with normal ctrl set as 1 or 0.1 ($n$ =3, *$P$ <0.001 versus normal WT group, $^{\#}P$ <0.01, NS: not significant).

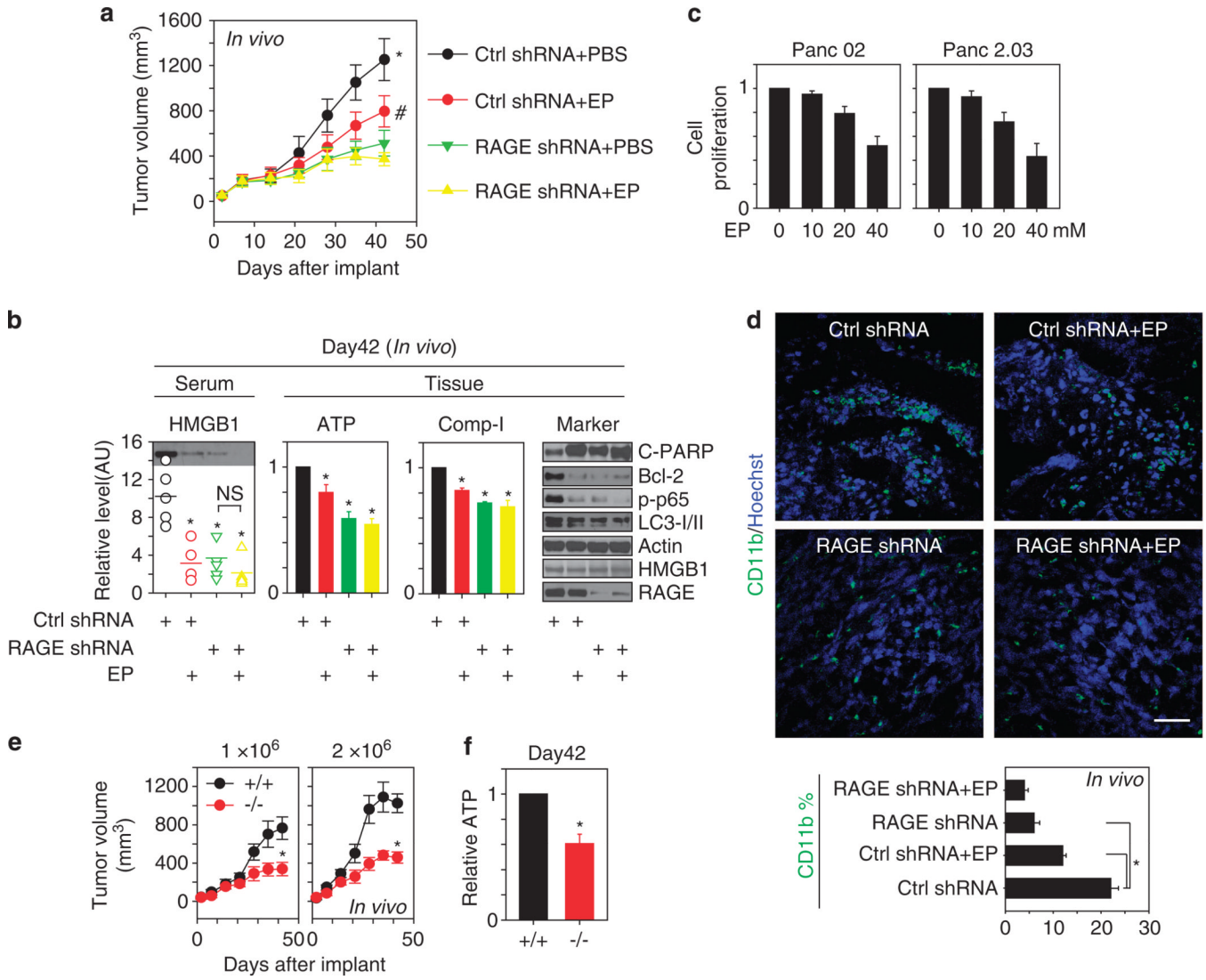


**Figure 5.**

RAGE is required for HMGB1-mediated ATP production. (**a**) C57/BLl6 mice were inoculated with $10^6$ Panc02 tumor cells following transfection of control or RAGE-specific shRNA and treated with an HMGB1 inhibitor, 'EP', 40 mg/kg, or PBS beginning on day 7. Tumors were measured twice weekly, and volumes were calculated for 42 days (mean ±s.d., $n = 5$, *$P<0.001$ ctrl shRNA versus RAGE shRNA; $^{\#}P<0.01$ ctrl shRNA versus ctrl shRNA + EP). (**b**) On day 42 in the experiments described in (**a**), serum HMGB1 (left) and protein levels of C-PARP, Bcl-2, p-p65 and LC3-I/II (right) in tumor samples were assayed by western blotting. The relative optical intensity of the HMGB1-immunoreactive band (in arbitrary units, AU) is shown in a scatter plot with the mean represented by a solid line ($n = 5$, *$P<0.001$ versus ctrl shRNA). The inset shows a representative western blot. In parallel, relative ATP levels and complex I activity in tumor tissue were evaluated, with ctrl shRNA set as 1 (mean ± s.d., $n = 3$, *$P$ <0.001 versus ctrl shRNA). **(c)** Dose-response effects of EP on cellular proliferation in Panc02 and Panc2.03 cells. (**d**) On day 42 as described in (**a**), the percentage of CD11b positive cells in tumor tissue was evaluated (mean ± s.d., $n=3$, *$P<0.001$). (**e**) RAGE wild-type (+/+) and knockout (−/−) mice were inoculated with 0.5–1 × $10^6$ Panc02 tumor cells. Tumors were measured twice weekly, and tumor volumes

calculated for 42 days (mean ± s.d., $n$=5, *$P$<0.001 +/+ versus −/−). (**f**) On day 42 described in (**e**), ATP levels in tumor tissue ($1 \times 10^6$) were determined, with normal RAGE wild-type (+/+) set as 1 (mean±s.d., $n$ = 3, *$P$<0.001 versus +/ +).

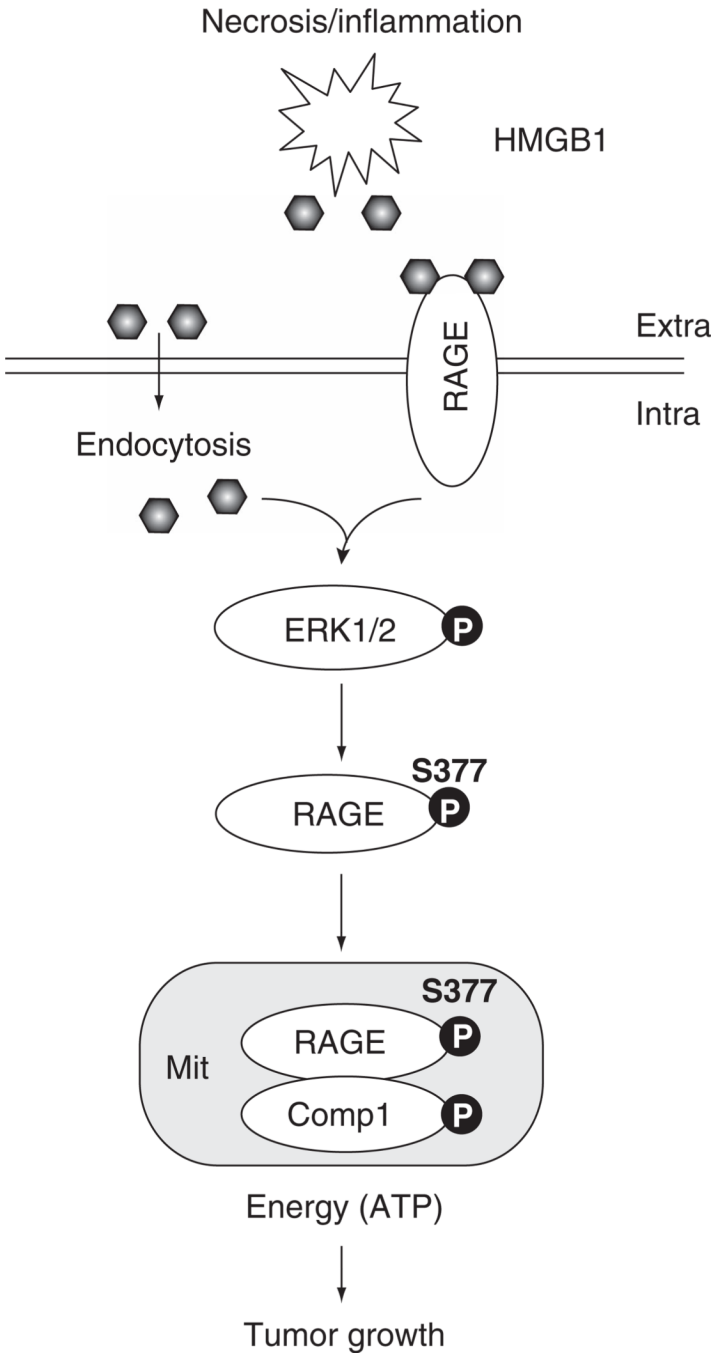


**Figure 6.**

Model of HMGB1/RAGE interaction and regulation of metabolism. HMGB1 is released following stress/necrosis in cells as a damage-associated molecular pattern molecule in the tumor microenvironment, promoting inflammation. HMGB1 binds cell membrane RAGE or uptake into cells by a caveolin-dependent endocytosis pathway, promoting phosphorylation of ERK1/2 (p-ERK1/2), which in turn induces phosphorylation of RAGE. Phosphorylation of RAGE at Ser377 is required for its mitochondria-targeted accumulation. There it promotes phosphorylation of complex I, which is the first step in the ATP biosynthetic pathway. As shown in the summary, the HMGB1–RAGE pathway stimulates bioenergetics

by enhancing ATP production in a p-ERK1/2-dependent process to sustain the increased metabolic needs and growth of tumor cells.